ISSN: 0871-7869

Generalized Pushover Curves for Nonlinear Static Analysis of Three-Dimensional Structures

C. Bhatt; R. Bento

- Março de 2012 -

Relatório ICIST
DTC nº 06/2012

Index

1. Introduction

The Nonlinear Static Procedures (NSP) have been accepted worldwide as a practical tool to estimate seismic demands in buildings, being included in different seismic codes (CEN, 2004; ASCE/SEI-41, 2007; ATC-40, 1996; FEMA-356, 2000; FEMA-440, 2005).

The first versions of the NSPs considered that the structural response was only influenced by the fundamental mode. Therefore, the applicability of these methods was limited to low-rise buildings. Several researchers developed studies in order to extend the applicability of such pushover analyses to structures where higher modes may contribute significantly to the response (Antoniou and Pinho, 2004a, 2004b; Aydinoglu, 2003; Bracci et al., 1997; FEMA-440, 2005; Gupta and Kunnath, 2000; Kalkan and Kunnath, 2006).

The most well known multi-modal pushover method is the Modal Pushover Analysis (MPA) procedure (Chopra and Goel, 2002, 2004; Goel and Chopra, 2004; Goel, 2005). This method was proven in several studies to lead to reliable and accurate seismic estimations in buildings where higher mode effects also play an important role.

It is important to mention that the pushover curve in the MPA and in the other NSPs is defined as a relationship between the base-shear, V_{bn}, and the lateral roof (or any other reference location) displacement, urn.

The Vbn − urn pushover curve is useful because it gives information about the base shear capacity of the building under study. However, in buildings that have participating modes involving torsional motion about a vertical axis, inducing little or no base shear, this type of curve may not provide important information.

Goel (2008) proposed an alternative and more robust definition of pushover curve and the procedure to convert it to the force-displacement relationship, F_{sn}

/ $L_n - D_n$, of the nth – mode of the inelastic SDOF system to be implemented in the MPA procedure. The author called it the Generalized Pushover Curve.

This report intends to evaluate the performance of the Generalized Pushover Curve proposed by Goel in a reinforced concrete three dimensional building.

The results obtained confirmed that the commonly used base-shear versus reference-location displacement pushover curve is a special case of the generalized pushover curve.

2. Generalized Pushover Curve

The steps of the Modal Pushover Analysis (MPA) procedure are described in several papers such as (Chopra and Goel, 2002, 2004; Goel, 2008).

The force distribution, f_s, to be applied in the nth mode pushover analysis in the MPA procedure is given by Eq. 1:

$$\mathbf{f}_s = \beta_n \mathbf{m} \boldsymbol{\phi}_n \qquad \text{Eq. 1}$$

Increasing intensities should be applied to the previous force pattern according to the force scale factor β_n .

In Goel (2008), the author proposes the so called Generalized Pushover Curve as a relationship between β_n and u_{rn}, where u_{rn} is the displacement at the reference location. The $F_{sn} / L_n - D_n$ force-deformation relationship of the nth mode inelastic SDOF system is computed from Eq. 2 and 3:

$$\frac{F_{sn}}{L_n} = \frac{\boldsymbol{\phi}_n^T \mathbf{f}_s}{L_n} \qquad \text{Eq. 2}$$

$$D_n = \frac{u_{rn}}{\Gamma_n \phi_{rn}} \qquad \text{Eq. 3}$$

Where, ϕ_n is the nth mode shape and ϕ_{rn} is the value of ϕ_n at the reference location. Γ_n is the modal participation factor of the nth mode given by Eq. 4 where m is the mass.

$$\Gamma_n = \frac{\boldsymbol{\phi}_n^T \mathbf{m} \boldsymbol{\iota}_e}{\boldsymbol{\phi}_n^T \mathbf{m} \boldsymbol{\phi}_n} \qquad \text{Eq. 4}$$

Using Eq. 1 and Eq. 2, one obtains:

$$\frac{F_{sn}}{L_n} = \frac{\boldsymbol{\phi}_n^T \mathbf{f}_s}{L_n} = \frac{\beta_n \boldsymbol{\phi}_n^T \mathbf{m} \boldsymbol{\phi}_n}{L_n} = \frac{\beta_n M_n}{L_n} = \frac{\beta_n}{\Gamma_n} \qquad \text{Eq. 5}$$

The generalized $\beta_n - u_{rn}$ pushover curve of a structure can be converted to the $F_{sn} / L_n - D_n$ curve of the inelastic SDOF system using Eq. 3 and Eq. 5. The modal participation factor, Γ_n, is defined according Eq. 4.

The Generalized Pushover Curve can only be developed for modes with a modal participation factor different than zero. The initial slope of the bilinear idealization of the $F_{sn} / L_n - D_n$ curve is equal to $2\omega_n$. Therefore, the vibration period T_n of the inelastic SDOF system can be calculated using Eq. 6, in which subscript *y* indicates the yield values.

$$T_n = 2\pi \left(\frac{L_n D_{ny}}{F_{sny}} \right)^{1/2} \qquad \text{Eq. 6}$$

This value of T_n, is used for estimating deformation of the inelastic SDOF system.

The commonly used pushover curve in buildings is the one that relates the base shear, V_{bn} , with the reference location displacement, u_{rn} . From this pushover curve, the F_{sn} / L_n curve for the *n*th mode SDOF system is computed using Eq. 7:

$$\frac{F_{sn}}{L_n} = \frac{V_{bn}}{M_n^*} \qquad \text{Eq. 7}$$

Where M_n^* is the effective translational mass in the *n*th mode defined in Eq. 8.

$$M_n^* = \frac{\left(\boldsymbol{\phi}_n^T \mathbf{m} \boldsymbol{\iota}_e \right)^2}{\boldsymbol{\phi}_n^T \mathbf{m} \boldsymbol{\phi}_n} \qquad \text{Eq. 8}$$

In a multi storey building, Eq. 7 is a special case of Eq. 5, which can be proven from Eq. 9 and 10.

$$V_{bn} = \mathbf{1}^T \mathbf{f}_{sn} = \beta_n \mathbf{1}^T \mathbf{m}\boldsymbol{\phi}_n = \beta_n \boldsymbol{\phi}_n^T \mathbf{m}\mathbf{1} = \beta_n L_n \quad \text{Eq. 9}$$

$$\frac{V_{bn}}{M_n^*} = \frac{V_{bn}}{\Gamma_n L_n} = \frac{\beta_n L_n}{\Gamma_n L_n} = \frac{\beta_n}{\Gamma_n} \quad \text{Eq. 10}$$

The pushover curve for an asymmetric building can also be plotted as a relationship of base torque, T_{bn} , and reference location rotation, θ_{rn} . This pushover curve can be converted to the $F_{sn} / L_n - D_n$ curve of the inelastic SDOF system by using Eq. 11 and Eq. 12.

$$\frac{F_{sn}}{L_n} = \frac{T_{bn}}{I_{on}^*} \quad \text{Eq. 11}$$

$$D_n = \frac{\theta_{rn}}{\Gamma_n \phi_{r\theta n}} \quad \text{Eq. 12}$$

Where I_{on}* is the effective rotational mass moment of inertia in the nth mode given by Eq. 13

$$I_{on}^* = \Gamma_n \mathbf{1}^T \mathbf{I}_o \boldsymbol{\phi}_{\theta n} \quad \text{Eq. 13}$$

and $\boldsymbol{I}_o$ is a matrix of mass moment of inertia of various floors of the building and $\boldsymbol{\phi}_{\theta n}$ *is* a vector of rotational mode shape components.

The $V_{bn} - u_{rn}$ pushover curve can give important information about base-shear or base-torque capacity of the building under analysis. However, in participating modes with torsional motions about a vertical axis inducing little or no base shear, these curves might not be useful. Therefore, the $\beta_n - u_{rn}$ *relationship* is a more robust pushover curve since the value of β_n is always different from zero during the pushover analysis for all types of modes. The $V_{bn} - u_{rn}$ pushover curve is a special case of $\beta_n - u_{rn}$ *Generalized* Pushover Curve.

3. Case Study

The case study used in this endeavor is the well known SPEAR building − an irregular 3D structure tested pseudo-dynamically in full-scale under bi-directional seismic loading in ELSA laboratory. The analytical model used in this study was calibrated with experimental results.

The analysed building represents a typical older three storey reinforced concrete frame building constructed in the Mediterranean region following the construction practice and materials used in Greece in the early 1970s. The structure was designed only to gravity loads, with no provisions for earthquake resistance, according to the concrete design code implemented in Greece between 1954 and 1995. It was experimentally and numerically investigated in the SPEAR project (an European project within 6th framework). The details of which can be found elsewhere (Fardis and Negro 2006, Fardis 2002). A schematic plan and elevation of the building is presented in Figure 1.

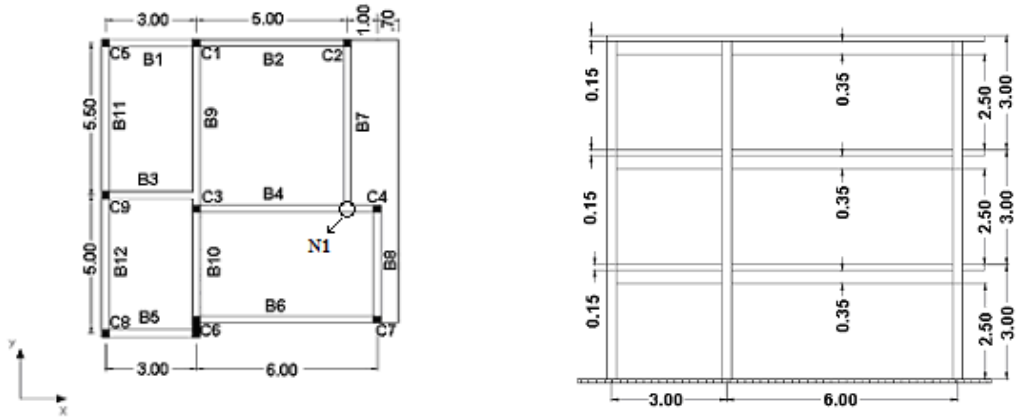

(a) (b)

Figure 1 - Building configuration: (a) in plan, (b) at the south west facade (units meters).

4. Numerical Modeling

4.1 General modeling strategy

The SPEAR building was modeled by an assemblage of inter-connected frame elements using centreline dimensions and incorporating distributed material inelasticity through displacement based formulation along with geometric nonlinearity utilizing corotational formulation. The storey heights amounted to 2.75 m for first floor and 3.00 m for upper stories. Each element was discretized into four sub-elements with two integration points each. Fiberized cross-sections − representing sectional details such as cover and core concrete and longitudinal reinforcements − were then defined at respective integration points, whereby every fiber was assigned to an appropriate material constitutive relationship, as described below. The sectional responses were obtained by integrating the material responses across a section using mid-point rule, whilst element-level responses were determined through Gauss-Lengendre integration scheme using section responses at integration points within the element. Further discussions can be found in (Calabrese et al. 2010). In order to keep the analytical model simple, the effect of beam-column joints, slippage and pullout of smooth reinforcing bars, etc. were not included in the model. Exclusion of these effects, as shown later, did not affect much on the accuracy of the results as verified from experimental data, but reduced significantly the analysis time. Further details about numerical modeling can be found elsewhere (Meireles et al. 2006). A freely downloadable fibre element based finite element program SeismoStruct (SeismoSoft 2006) was employed to perform all the aforementioned pushover analyses as well as the nonlinear dynamic analyses for comparison with experimental results.

4.2 Materials

The constitutive relationship proposed by Mander et al. (1988) along with the cyclic rules introduced by Martinez-Rueda and Elnashai (1997) was deployed to model the behavior of unconfined concrete. In absence of sufficient transverse reinforcement, the confinement effects were not considered for core concrete. The mean compressive strength of unconfined concrete was taken as 25 MPa. The constitutive model used for the steel was proposed by Menegotto and Pinto (1973) including the modifications due to isotropic hardening proposed by Filippou et al. (1983). An average yield strength of 360 MPa and ultimate strength of 450 MPa were assumed for reinforcements.

4.3 Mass and loading

A lumped mass modeling strategy was adopted, in which masses were lumped at the nodal points according to its tributary area. Total translational masses amounted to 67.3 tonnes each for first two floors and 62.8 tonnes for the roof. The eccentric disposition of centre of rigidity (CR) with respect to centre of mass (CM) of each floor, by distances of 1.3 m and 1.0 m along the x− and y− axis respectively, effectively rendered the structure as irregular, according to the criteria set forth by Eurocode 8 (CEN 2004). The sustained gravity loads were automatically computed by the software, using the defined masses.

4.4 Diaphragm Modeling

The floor slabs of the building possessed very high in-plane stiffness compared to the out-of-plane (flexural) one and thus can safely be modeled as ‘rigid diaphragm’. In the present work, such diaphragms were modeled by imposing kinematic constraints on the lateral displacements of all nodes at each floor so that they (nodal displacements) can be expressed by three rigid body motions of the respective floors, namely two horizontal translations and one rotation about the normal to the floor-plane. This reduces significantly the number of

dynamic degrees of freedom and hence increases the efficiency for large parametric studies. The effects of flexural stiffness of slab were considered by assigning appropriate flange widths to the beams. Further details about relative accuracy of other slab modeling approaches can be found elsewhere (Pinho, Bhatt, Antoniou and Bento 2008).

5. Comparison with experimental results

The SPEAR building was pseudo-dynamically tested (Figure 2(a)) with a bi-directional loading based on a ground motion recorded at Hercegnovi station during the 1979 Montenegro earthquake and scaled to match with the EC8 type I spectrum for soil type C. This bi-directional record was applied to the structure in three runs of linearly increasing intensity of peak ground acceleration (pga), such as 0.02 g, 0.15 g and 0.20 g. The very same input motion was used to authenticate the adequacy of the current analytical model, so that the same model can be used for further studies with confidence.

(a) (b)

Figure 2 - SPEAR building: (a) Experiment specimen, (b) Analytical model.

Figure 3 shows a comparison between experimental and analytical results for displacement histories at two orthogonal directions. Despite being a simplified analytical model, it reproduced the experimental results with appreciable accuracy. The observed discrepancies are due to the lack of various modeling aspects, like beam-column joints, slippage and pull-out of smooth reinforcing bars, etc., incorporation of which into the current model would increase considerably the computation time. The current analytical model provides

perhaps the best trade-off between accuracy and efficiency; and therefore used for the further analyses.

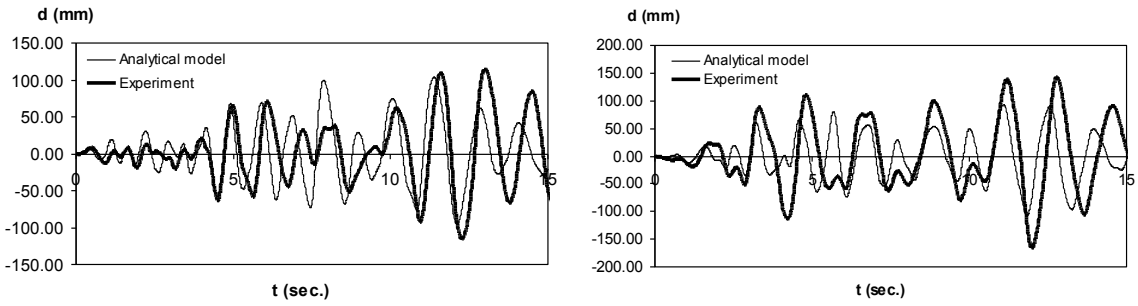

(a) (b)

Figure 3 - (a) Top displacement in node C7, X direction, (b) Top displacement in node N1, Y direction.

The software used in this study takes into account both material inelasticity and geometric nonlinearities, although the authors tend to feel that the P-delta effects are likely not to play a critical role in the response of structures such as the one considered in this study.

6. Dynamic Properties

In Figure 4 are represented the modes of vibration of the case study analysed.

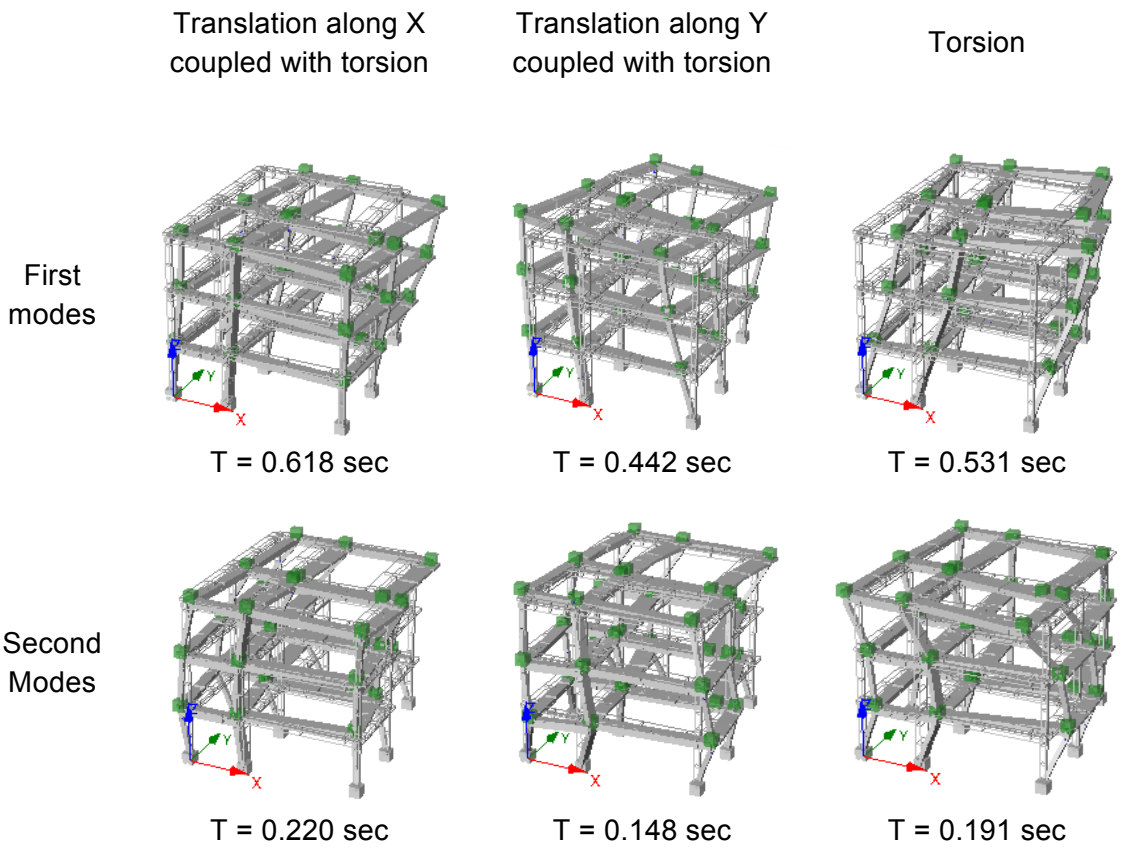

Figure 4 – Modes of vibration of the SPEAR building.

The modes of vibration that exhibit translational motions are coupled with torsion. This fact turns the building torsional sensitive, therefore it should be analysed using a 3D model.

7. Pushover Curves of the SPEAR Building

The pushover curves for the first and the second coupled modes along X and Y directions of the SPEAR building and the conversion of these pushover curves to the F_{sn} / L_n − D_n curve for the corresponding inelastic SDOF system are presented in this section.

In each figure (from Figure 5 to 8) are presented first the V_{bn} − u_{rn} pushover curve (base shear versus displacement at the reference location) and the Generalized β_n − u_{rn} Pushover Curve for each of the selected modes. These two curves are converted to the F_{sn} / L_n − D_n curve using the appropriate transformation equations described in section 2.

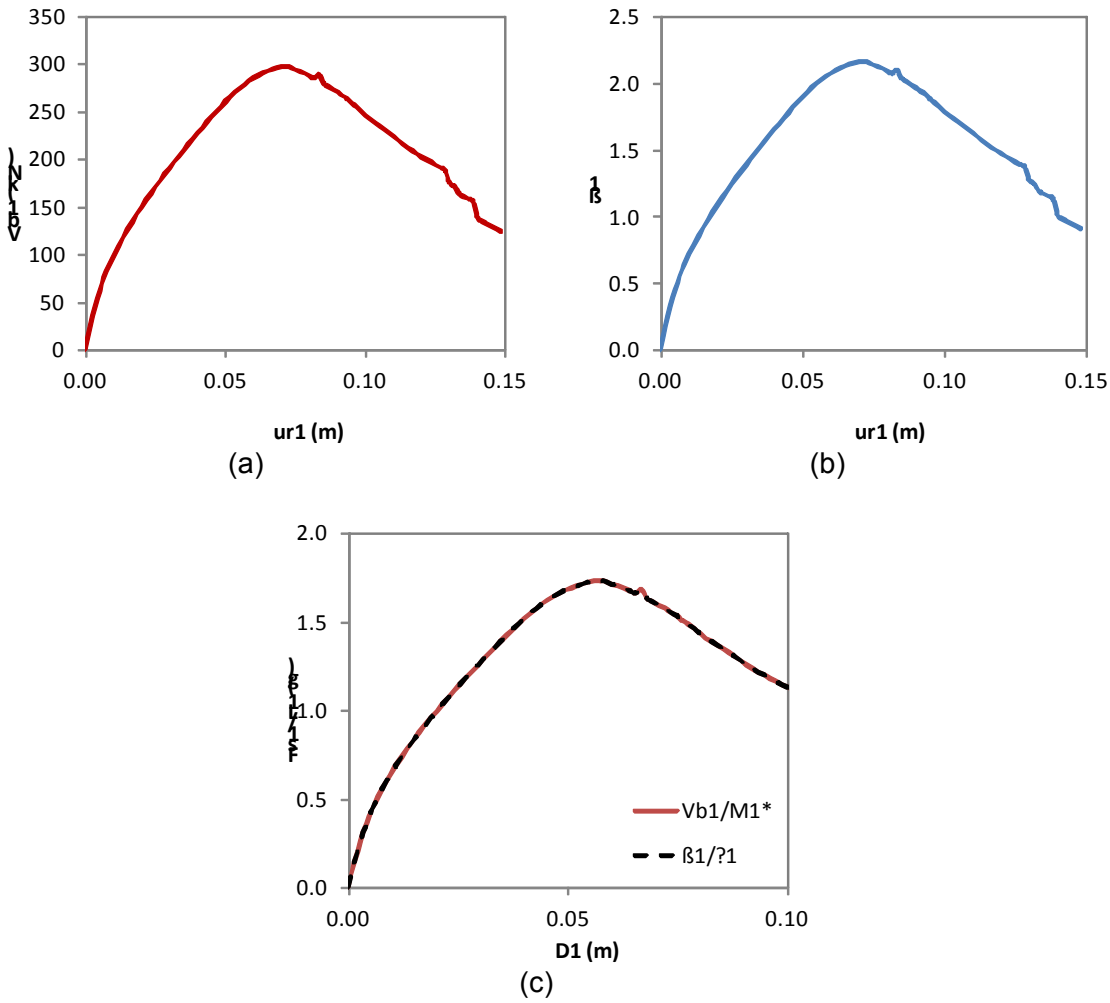

Figure 5 - Pushover curves for 1st coupled mode along the X direction (T=0.618sec): (a) V_{bn} − u_{rn} pushover curve; (b) β_n − u_{rn} pushover curve; (c) F_{sn} / L_n − D_n curve.

In Figure 5 are represented the pushover curves for the first coupled mode with translation along the X direction.

In Figure 6 are represented the pushover curves for the second coupled mode with translation along the X direction.

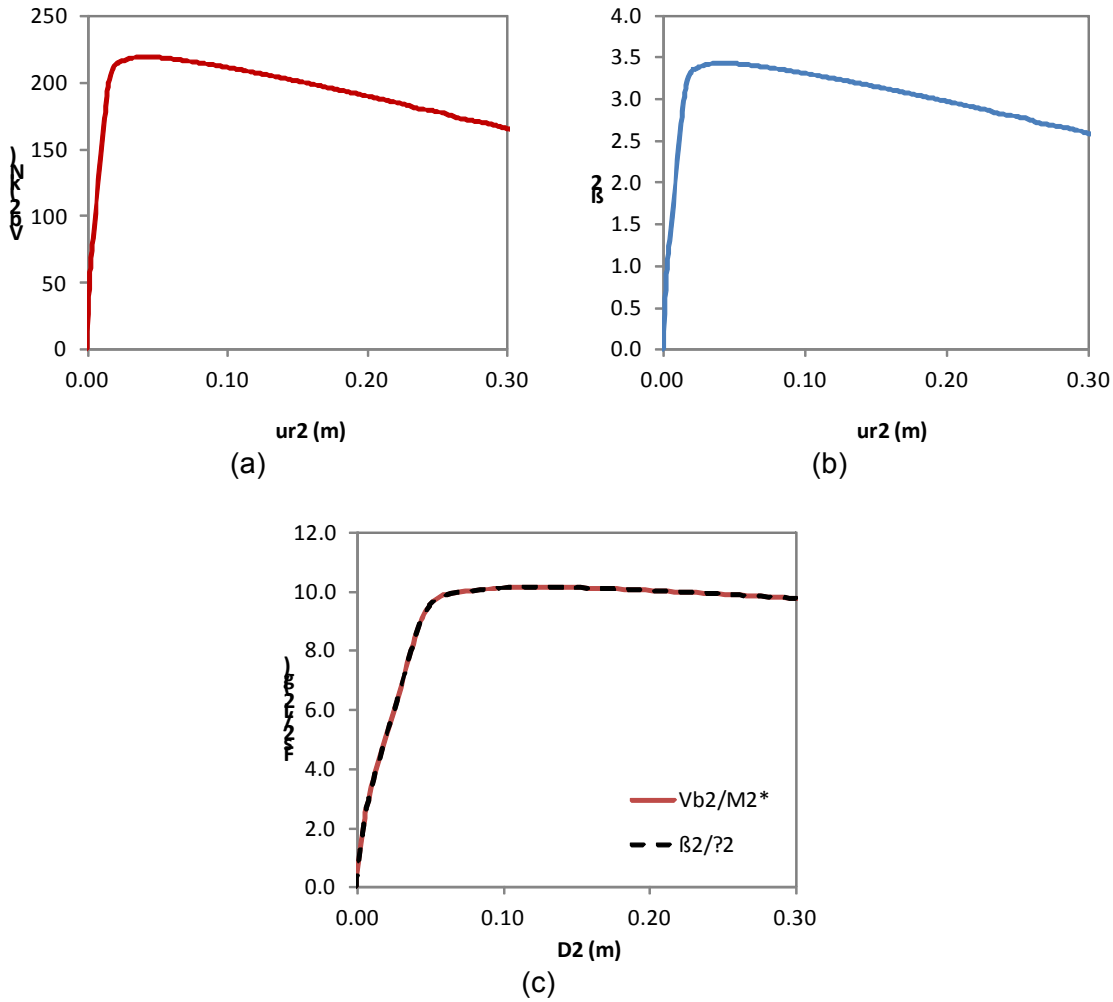

Figure 6 - Pushover curves for 2nd coupled mode along the X direction (T=0.220sec): (a) $V_{bn} - u_{rn}$ pushover curve; (b) $\beta_n - u_{rn}$ pushover curve; (c) $F_{sn} / L_n - D_n$ curve.

In Figure 7 are represented the pushover curves for the first coupled mode with translation along the Y direction.

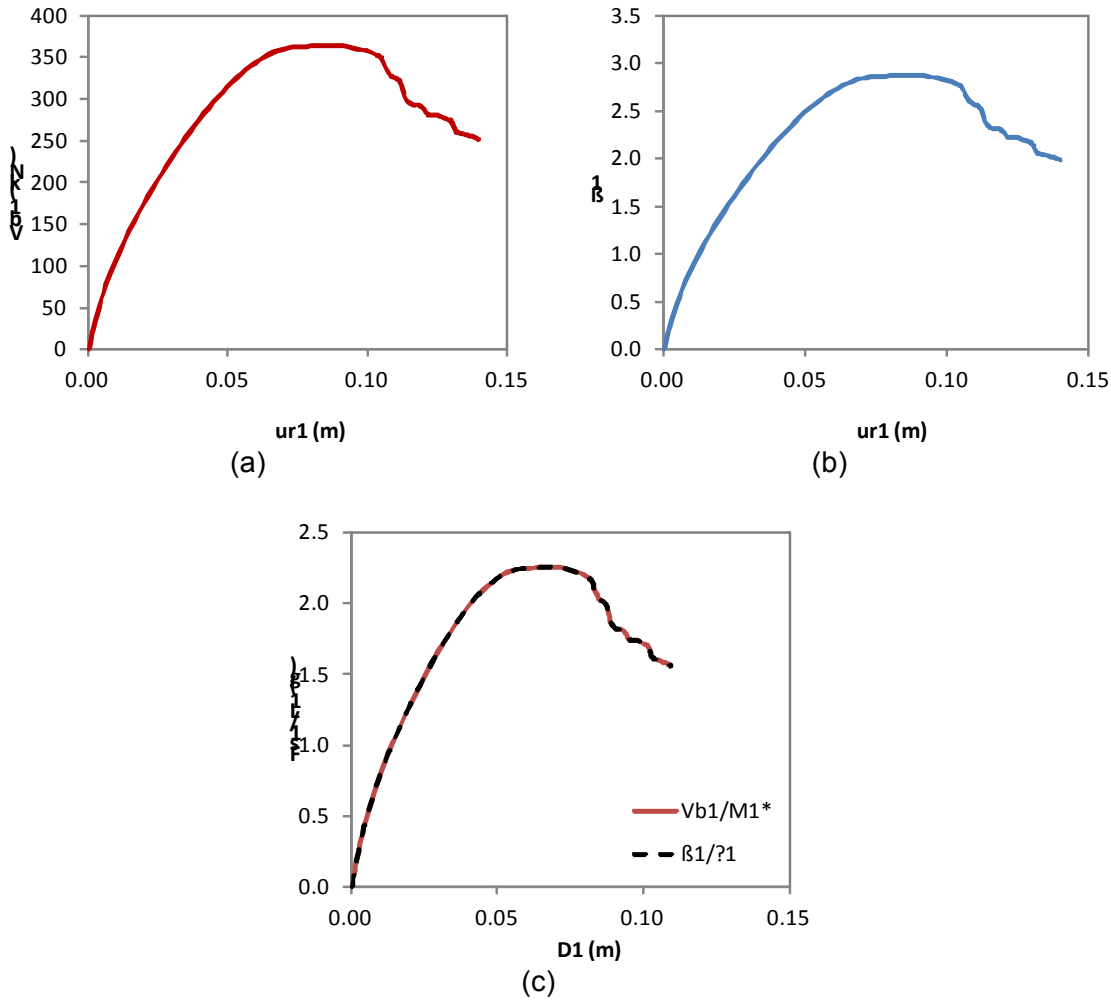

Figure 7 - Pushover curves for 1st coupled mode along the Y direction (T=0.442sec): (a) $V_{bn} - u_{rn}$ pushover curve; (b) $\beta_n - u_{rn}$ pushover curve; (c) $F_{sn} / L_n - D_n$ curve.

In Figure 8 are represented the pushover curves for the second coupled mode with translation along the Y direction.

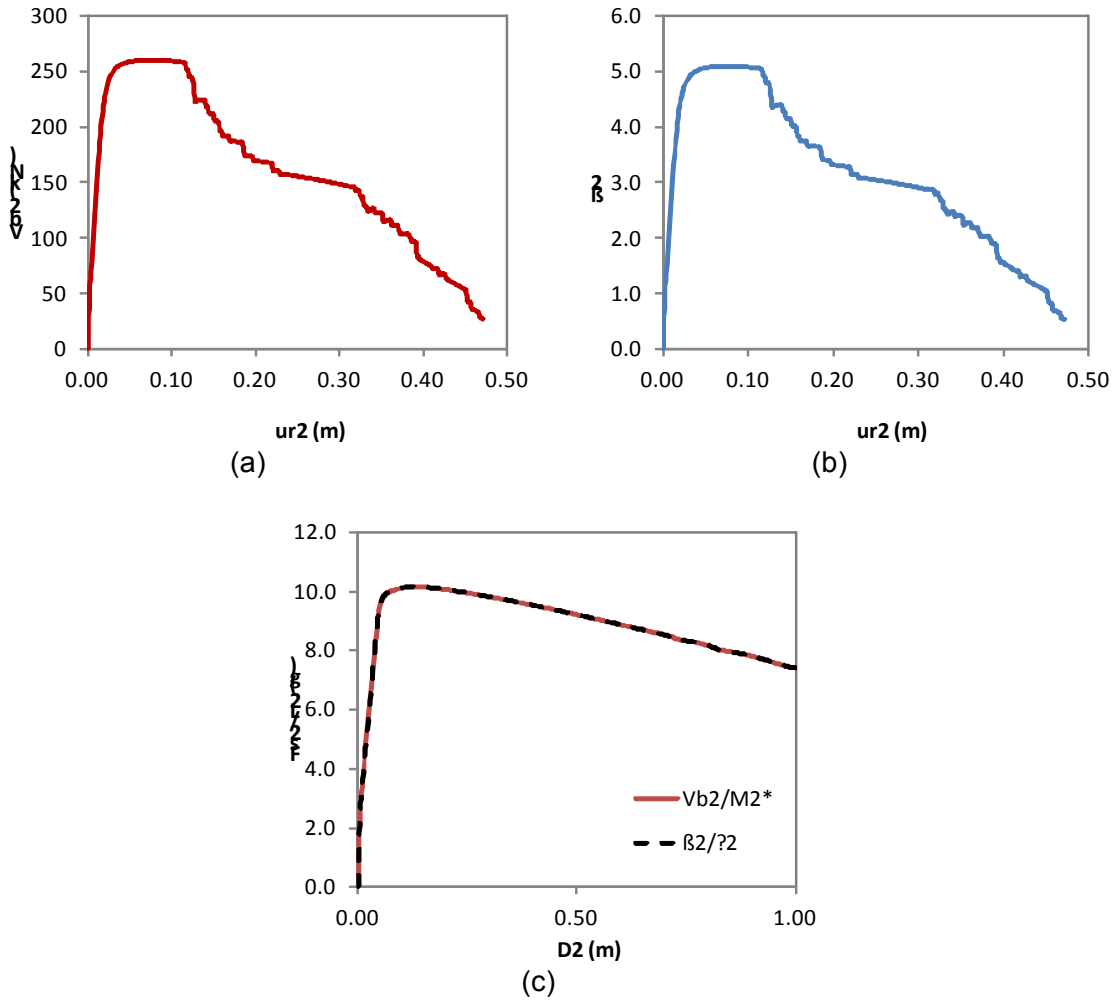

Figure 8 - Pushover curves for 2nd coupled mode along the Y direction (T=0.148sec): (a) $V_{bn} - u_{rn}$ pushover curve; (b) $\beta_n - u_{rn}$ pushover curve; and (c) $F_{sn} / L_n - D_n$ curve.

From figures 5 to 8 one can conclude that the Generalized $\beta_n - u_{rn}$ Pushover Curve transformed by equations 3 and 5 lead to the same $F_{sn} / L_n - D_n$ curve of the *n*th mode inelastic SDOF system as the commonly used $V_{bn} - u_{rn}$ pushover curve (base shear versus displacement at the reference location) transformed by equations 3 and 7.

In Goel (2008), the author also demonstrates that for a certain *n*th coupled transverse-torsional mode the $T_{bn} - \theta_{rn}$ pushover curve (base torque versus rotation at the reference location) transformed by equations 11 and 12 and the Generalized $\beta_n - \theta_{rn}$ Pushover Curve transformed by equations 3 and 5 lead to the same $F_{sn} / L_n - D_n$ curve of the *n*th mode inelastic SDOF system. These conclusions are confirmed in Figures 9 and 10.

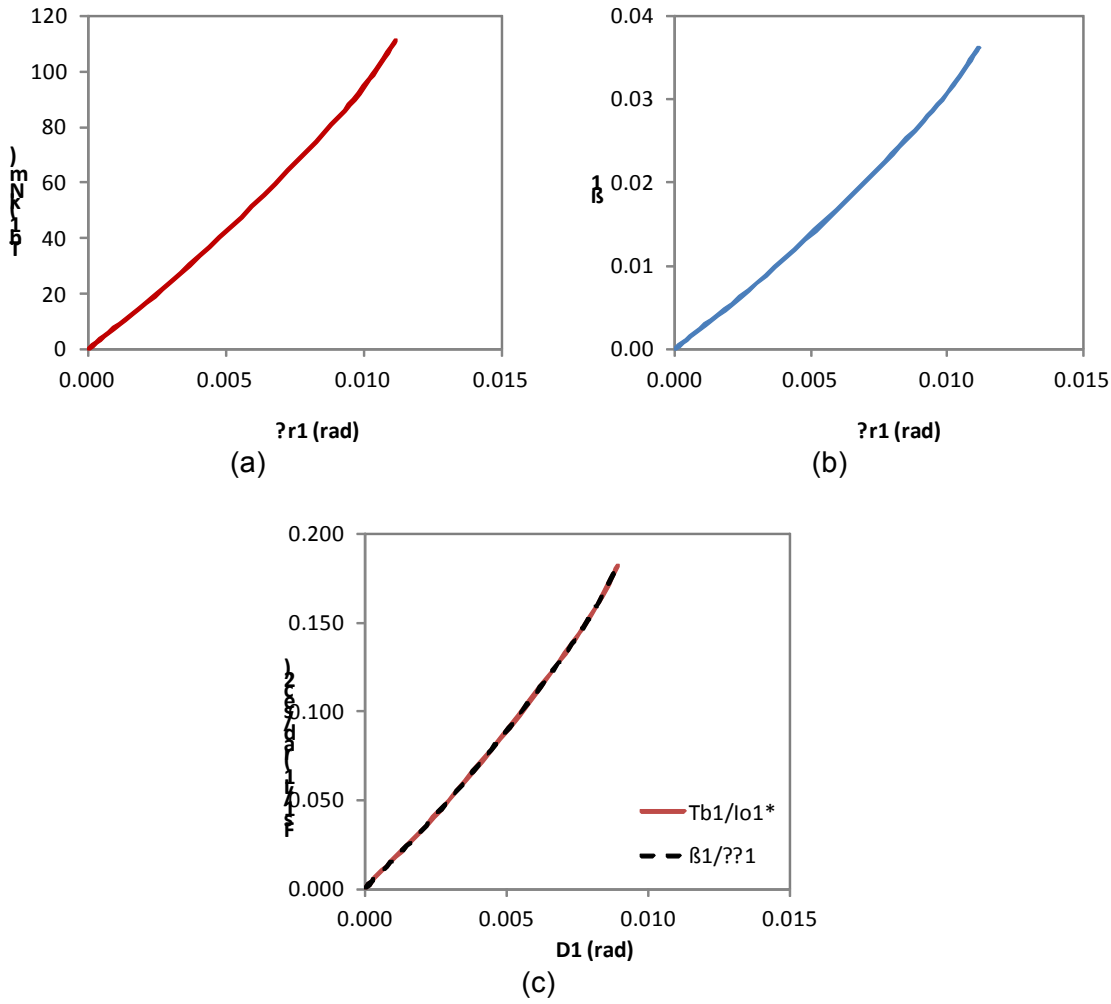

Figure 9: Pushover curves for 1st coupled mode along the X direction (T=0.618sec): (a) $T_{bn} - \theta_{rn}$ pushover curve; (b) $\beta_n - \theta_{rn}$ pushover curve; (c) $F_{sn} / L_n - D_n$ curve.

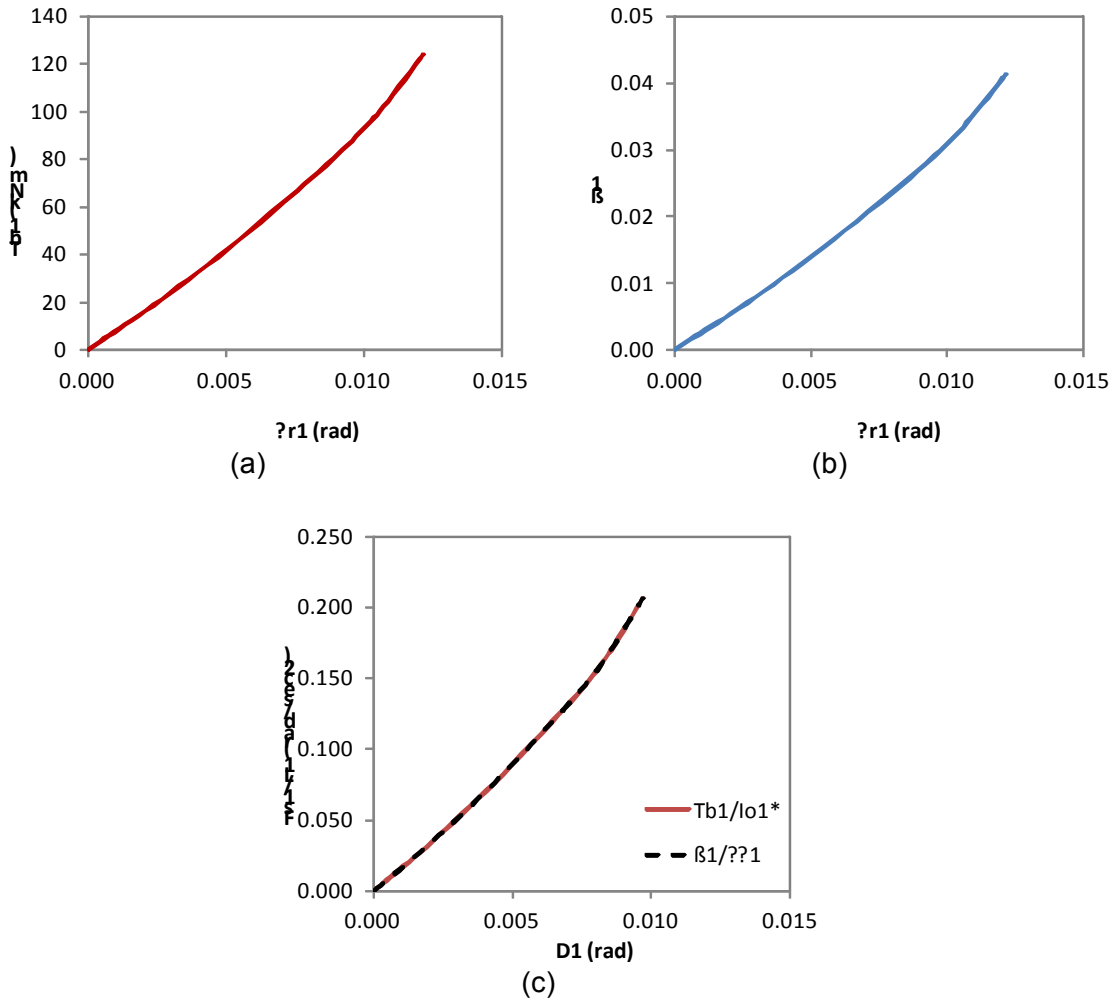

Figure 10: Pushover curve for 1st coupled mode along the Y direction (T=0.442sec): (a) $T_{bn} - \theta_{rn}$ pushover curve; (b) $\beta_n - \theta_{rn}$ pushover curve; (c) $F_{sn} / L_n - D_n$ curve.

The results show that both $T_{bn} - \theta_{rn}$ pushover curve and $\beta_n - \theta_{rn}$ Generalized Pushover Curve lead to the same $F_{sn} / L_n - D_n$ curve.

The conclusions drawn in this report about the Generalized Pushover Curve are justified by the theoretical background presented in section 2.

These results corroborate the ones presented in Goel (2008) for a 13-story Commercial Building in Sherman Oaks, USA.

It is expected that for a certain *n*th coupled mode, the $F_{sn} / L_n - D_n$ curve generated either from the $V_{bn} - u_{rn}$ pushover curve or from the $T_{bn} - \theta_{rn}$ pushover curve are essentially identical (Goel 2008). However, in this work the pushover curves base torque versus rotation at the reference location could not be completed, because the software found numerical problems during the analyses. For this reason, further conclusions on this issue cannot be taken herein.

8. Conclusions

This report has the objective of testing the proposal of Goel (2008) on the definition of the Generalized Pushover Curve to 3D buildings. The rules to transform them to the force-deformation relationships of the inelastic SDOF system were also verified herein. These curves are to be used in the Modal Pushover Analysis or in any other Nonlinear Static Procedure.

The Generalized Pushover Curve relates the scaling factor, β_n, applied to the nth mode pushover force distribution, $f_s = \beta_n m \varphi_n$, with the translational or rotational displacement, u_{rn}, at a certain reference location.

The Generalized Pushover Curve can be used in 3D buildings for modes that may induce little or no base shear, because it does not explicitly need the base shear.

The case study used in this work was the three storey reinforced concrete SPEAR building, asymmetric in plan. The modeling options were calibrated through comparison with the experimental test at ELSA laboratory.

The Generalized Pushover Curve was tested in the SPEAR building and compared with the commonly used $V_{bn} - u_{rn}$ (base shear versus displacement at the reference location) or $T_{bn} - \theta_{rn}$ (base torque versus rotation at the reference location) pushover curves. As it is concluded in Goel (2008), it was confirmed in this report that the two types of pushover curves lead to the same force-deformation relationship of the inelastic SDOF system. These results can be justified by the theoretical background associated to their definition and presented in section 2.

Moreover, one can conclude that the $V_{bn} – urn$ pushover curve is a special case of the Generalized $\beta_n - u_{rn}$ Pushover Curve.

Acknowledgements

The authors would like to special acknowledge Professor Rakesh Goel for the valuable discussions regarding the implementation of the Generalized Pushover Curve, which certainly enriched the work herein presented. The authors would like to acknowledge the financial support of the Portuguese Foundation for Science and Technology (Ministry of Science and Technology of the Republic of Portugal) through the research project PTDC/ECM/100299/2008 and through the PhD scholarship SFRH/BD/28447/2006 granted to Carlos Bhatt.

References

Antoniou, S. and Pinho, R., 2004a. Advances and Limitations of Adaptive and Non-Adaptive Force- Based Pushover Procedures, *Journal of Earthquake Engineering*, 8(4): 497-522.

Antoniou, S. and Pinho, R., 2004b. Development and Verification of a Displacement-Based Adaptive Pushover procedure, *Journal of Earthquake Engineering*, 8(5): 643-661.

ASCE/SEI-41, 2007. Seismic Rehabilitation of Existing Building, *ASCE Standard No. ASCE/SEI 41-06,* American Society of Civil Engineers, Reston, VA.

ATC-40, 1996. *Seismic Evaluation and Retrofit of Concrete Buildings*, volumes 1 and 2, *Report No. ATC-40,* Applied Technology Council, Redwood City, CA.

Aydinoglu, M., 2003. An Incremental Response Spectrum Analysis Procedure on Inelastic Spectral Displacements for Multi-Mode Seismic Performance Evaluation, *Bulletin of Earthquake Engineering*, 1:3-36.

Bracci, J.M., Kunnath, S.K. and Reinhorn, A.M., 1997. Seismic Performance and Retrofit Evaluation for Reinforced Concrete Structures, *Journal of Structural Engineering*, 123(1):3-10.

Calabrese, A., Almeida, J. P. and Pinho, R., 2010, Numerical issues in distributed inelasticity modeling of RC frame elements for seismic analysis, *Journal of Earthquake Engineering*, 14(1). (in press)

Chopra, A.K., and Goel, R.K., 2002. A Modal Pushover Analysis Procedure for Estimating Seismic Demands for Buildings, *Earthquake Engineering and Structural Dynamics*, 31(3):561-582.

Chopra, A.K., and Goel, R.K., 2004. A Modal Pushover Analysis Procedure for Estimating Seismic Demands for Unsymmetric-Plan Buildings, *Earthquake Engineering and Structural Dynamics*, 33(3):903-927.

Comité Européen de Normalisation (CEN), 2004. *Eurocode 8: Design of structures for earthquake resistance. Part 1: general rules, seismic actions and rules for buildings*. EN 1998-1:2004, Brussels, Belgium.

Fajfar, P., Marusic, D. and Perus, I., 2005. Torsional effects in the pushover-based seismic analysis of buildings, *Journal of Earthquake Engineering*, 9(6), 831-854.

Fardis, M.N. and Negro, P., 2006. SPEAR - seismic performance assessment and rehabilitation of existing buildings, *Proceedings of the International Workshop on the SPEAR Project*, Ispra, Italy.

Fardis, M.N., 2002. Design of an irregular building for the SPEAR project - description of the 3 storey structure", *Research Report*, University of Patras, Greece.

FEMA 356, 2000. *Prestandard and Commentary for the Seismic Rehabilitation of Buildings*, FEMA Publication No. 356, prepared by the American Society of Civil Engineers for the Federal Emergency Management Agency, Washington, D.C.

FEMA-440, 2005. *Improvement of Nonlinear Static Seismic Analysis Procedures*, prepared by Applied Technology Council for Department of Homeland Security, Federal Emergency Management Agency, Washington, D.C.

Filippou, F.C., Popov, E.P. and Bertero, V.V., 1983. Modeling of R/C joints under cyclic excitations, *J. Struct. Eng.*, 109(11), 2666-2684.

Goel, R. K., 2005. Evaluation of Modal and FEMA Pushover Procedures Using Strong-Motion Records of Buildings, *Earthquake Spectra,* 21(3): 653-684.

Goel, R. K., 2008. Generalized Pushover Curves for Nonlinear Static Analysis of Three-Dimensional Structures, *Nonlinear Static Methods for Design/Assessment of 3D Structures,* Editors: R. Bento and R. Pinho, IST Press, ISBN 978-972-8469-76-4, pp. 1-14.

Goel, R. K., and Chopra, A.K., 2004. Evaluation of Modal and FEMA Pushover Analysis: SAC Buildings, *Earthquake Spectra,* 20(1): 225-224.

Gupta, B. and Kunnath, S.K., 2000. Adaptive Spectra-Based Pushover Procedure for Seismic Evaluation of Structures, *Earthquake Spectra*, 16(2):367 392.

Kalkan, E. and Kunnath, S. K., 2006. Adaptive Modal Combination Procedure for Nonlinear Static Analysis of Building Structures, *Journal of Structural Engineering,* 132(11): 1721-1731.

Mander, J.B., Priestley, M.J.N. and Park, R., 1988. Theoretical stress-strain model for confined concrete, J. *Struct. Eng. - ASCE*, 114(8), 1804-1826.

Martinez-Rueda, J.E. and Elnashai, A.S., 1997. Confined concrete model under cyclic load, *Mater. Struct*., 30(197), 139-147.

Meireles, H., Pinho, R., Bento, R. and Antoniou, S., 2006. Verification of an adaptive pushover technique for the 3D case, *Proceedings of 13th European Conference on Earthquake Engineering*, Switzerland, 619.

Menegotto, M. and Pinto, P.E., 1973. Method of analysis for cyclically loaded RC plane frames including changes in geometry and non-elastic behaviour of elements under combined normal force and bending, *Symposium on the Resistance and Ultimate Deformability of Structures anted on by well defined loads, International Association for Bridge and Structural Engineering*, Zurich, Switzerland, 15-22.

Pinho, R., Bhatt, C., Antoniou S. and Bento, R., 2008. Modeling of the horizontal slab of a 3D irregular building for nonlinear static assessment, *Proceedings of the 14th World Conference on Earthquake Engineering*, Beijing, China, 05-01-0159.

SeismoSoft, 2006. SeismoStruct - a computer program for static and dynamic nonlinear analysis of framed structures, Available online from URL: www.seismosoft.com.